ISSN 1063-7826, Semiconductors, 2022, Vol. 56, No. 3, pp. 234–239. © Pleiades Publishing, Ltd., 2022.

Comparison of Thin Films of Titanium Dioxide Deposited by Sputtering and Sol–Gel Methods for Waveguiding Applications

M. Brella[a], A. Taabouche[b,c,*], B. Gharbi[a,c], R. Gheriani[a], Y. Bouachiba[d], A. Bouabellou[b], H. Serrar[e], S. Touil[d], K. Laggoune[e], and M. Boudissa[f]

[a] *Laboratoire de Rayonnement et Plasmas et Physique des Surfaces (LRPPS), Université Kasdi Merbah, Ouargla, 30000 Algeria*

[b] *Thin Films and Interfaces Laboratory, University of Fréres Mentouri Constantine, Constantine, 25000 Algeria*

[c] *Faculty of Hydrocarbons and Renewable Energies and Earth and Universe Sciences, University Kasdi Merbah, Ouargla, 30000 Algeria*

[d] *Laboratoire Technologie des Matériaux Avancés, Ecole Nationale Polytechnique de Constantine Malek BENNABI, BP 75A RP Ali Mendjeli—Constantine, Algerie*

[e] *Research Center in Industrial Technologies (CRTI), BP 64 Cheraga (Alger), Algeria*

[f] *ENMC Laboratory, Department of Physics, Faculty of Sciences, University Ferhat Abbas, Setif, 19000 Algeria*

**e-mail: Adelphm@gmail.com*

Received November 11, 2020; revised November 11, 2020; accepted January 20, 2021

Abstract—In this work, TiO_2 thin films were deposited onto glass substrate by two different techniques: sol–gel dip-coating (SG) and reactive DC magnetron sputtering (Sput). The prepared samples have been characterized by means of micro-Raman, differential scanning calorimetry (DSC), thermogravimetric analysis (TGA) measurements, scanning electron microscopy (SEM), UV-Visible spectrophotometry, and M-Lines spectroscopy (MLS). The micro-Raman results showed an amorphous TiO_2-SG phase and the vibrational mode of TiO_2-Sput is anatase phase. DSC-TGA analysis was used to investigate the thermal properties of the TiO_2 material. SEM spectroscopy has shown that TiO_2-SG has a disordered and more porous surface, TiO_2-Sput sample is homogeneous and shows uniform distribution of densely packed well-defined grains. The obtained films have an optical transmittance varying from 60 to 88% in the visible region. The optical band gaps deduced from the transmittance are 3.48 and 3.53 eV for TiO_2-SG and TiO_2-Sput, respectively. The optical waveguiding measurements carried out on TiO_2-SG and TiO_2-Sput films show single guided modes behavior (TE_0 and TM_0). These measurements have allowed deducing the refractive index and thickness values that are 2.06 at 216 nm for TiO_2-SG and 2.26 at 204 nm for TiO_2-Sput thin films. The analysis of waveguiding properties indicates that amorphous TiO_2 may prove to be more efficient in photonic device as compared to crystalline TiO_2.

Keywords: TiO_2, thin films, sol–gel, sputtering, anatase, waveguiding

DOI: 10.1134/S106378262106004X

1. INTRODUCTION

Titanium dioxide (TiO_2) is one of the most studied transition metal oxides. TiO_2 have several advantageous properties such as availability, low cost, high refractive index, excellent optical transmittance in the visible and near IR regions, and large band gap of 3.5 eV compared to traditional semiconductors (1–1.5 eV), and good thermal stability [1, 2]. TiO_2 is found in three different phases rutile, brookite, and anatase. While rutile is the moste stable phase, both brookite and anatase are metastable. And these are good for industrial applications [3, 4].

These properties make them attractive materials for several applications such as antireflective coating, photocatalytic processes, solar cells, photovoltaic, optoelectronic [4–6], optical filter, and planar waveguides [1, 2].

In integrated optics, various applications are based on the use of transparent metal–oxide semiconductors thin-film planar waveguides. The approach to use TiO_2 films for the realization of such waveguide structures will be reported in the present paper.

Titanium dioxide can be grown as a thin film by physical or chemical deposition techniques, such as chemical vapor deposition, atomic layer deposition, beam evaporation [7–9], spray pyrolysis, sol–gel [10–12], and sputtering techniques [13]. Most TiO_2 thin films are prepared using chemical processes such as the sol-gel methods, mainly due to the advantages of simple equipment requirements, low cost, and the ease with which large or complicated surfaces can be

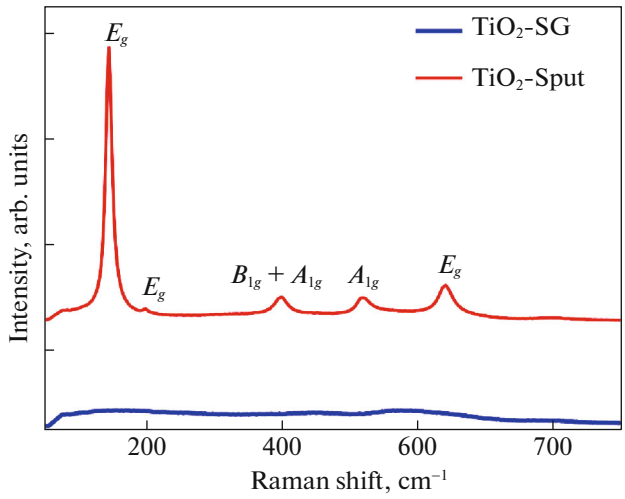

Fig. 1. Micro-Raman spectra of the TiO_2 thin films elaborated by sol–gel (SG) and sputtering (Sput) processes and annealed at 350°C.

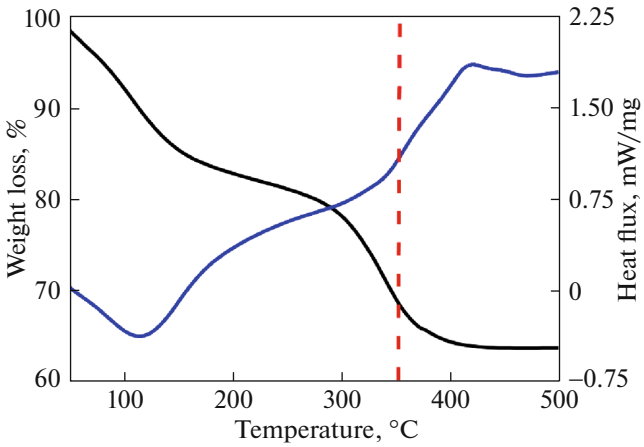

Fig. 2. DSC and TGA graphs for synthesized TiO_2 xerogel powder.

coated. The sputtering method has some advantages over chemical processes, namely, its simplicity (it is a one-step process) and the easy control of film thickness. Due to these significant advantages, there has been a recent widespread interest in TiO_2 thin films waveguiding.

The aim of this paper is to compare structural, morphological, and optical properties of TiO_2 thin films deposited by two different methods, namely, physical "reactive DC magnetron sputtering" and chemical "sol–gel dip-coating (SG)" for waveguiding applications.

2. EXPERIMENTAL PROCEDURES

The titanium thin film sample was deposited by reactive sputtering process (abbreviated as TiO_2-Sput) with a metallic Ti target of 99.99% purity onto microscope glass slides as substrate, the distance between the target and substrate was kept at 5 cm. The working gas used was a 1/2 mixture of Ar/O_2. The deposition rate was 5 nm/min. The sputtering power of the cathode was 150 W. The deposition film was annealed at 350°C.

Another sample (denoted as TiO_2-SG) was prepared through the sol-gel process using dip-coating procedure. The procedure of preparation includes the dissolution of titanium isopropoxide ($Ti(OC_3H_7)_4$) from Aldrich (97%) in isopropanol alcohol ($((CH_3)_2CHOH)$) by adding drop by drop. The solution was left under closed stirring during 15 min. Then, acetic acid was poured and stirred during 30 min. Finally, methanol was added and stirred during one hour. Thus obtained solution is transparent, of yellowish color, and is ready for deposit. The glass sample carefully cleaned was dipped into the solution and pulled up at constant rate. This thin film was dried for 15 min at 100°C and annealed at 350°C for 90 min. Micro-Raman analyses were recorded using Horiba Jobin Yvon HR800 instrument at excitation wavelength of 473 nm. The microstructure and morphologies were investigated by scanning electron microscopy (JEOL JSM-7001F model SEM) with an accelerating voltage of 4 kV. Differential scanning calorimetry (DSC) and thermogravimetric analysis (TGA) measurements were performed in order to study the thermal properties of the TiO_2 sample. They were performed simultaneously for TiO_2 sample, with a Jupiter STA 449 F3 calorimeter by NETZSCH. The optical transmittance spectra of TiO_2 thin films were recorded in the wavelength range of 300–800 nm by Shimadzu-3101PC UV–Vis spectrophotometer. The waveguiding properties (refractive index and guided modes) of TiO_2 thin films were investigated by a Metricon 2010/M prism coupler. The profiles of guided modes are obtained by measuring the refracted intensity a (He–Ne) laser beam operating at $\lambda = 632$ nm, as a function of incidence angle.

3. RESULTS AND DISCUSSION

3.1. Structural Analysis

It is well known that the anatase phase of TiO_2 has tetragonal structure with space group D_{4h}^{19} ($I4_1/amd$) [14, 15]. Overall, anatase has six modes of active bands for the Raman spectrum, which are ($A_{1g} + 2B_{1g} + 3E_g$), three modes ($A_{1u} + 2E_u$) are IR, and (B_{2u}) will be inactive vibration in both IR and Raman spectra [16, 17]. The samples of TiO_2 deposited onto glass substrates by sol-gel and sputtering processes annealing at 350°C were investigated by micro-Raman spectroscopy, which is presented in Fig. 1.

The TiO_2-Sput micro-Raman spectrum displays six symmetric modes of vibration bands identified at

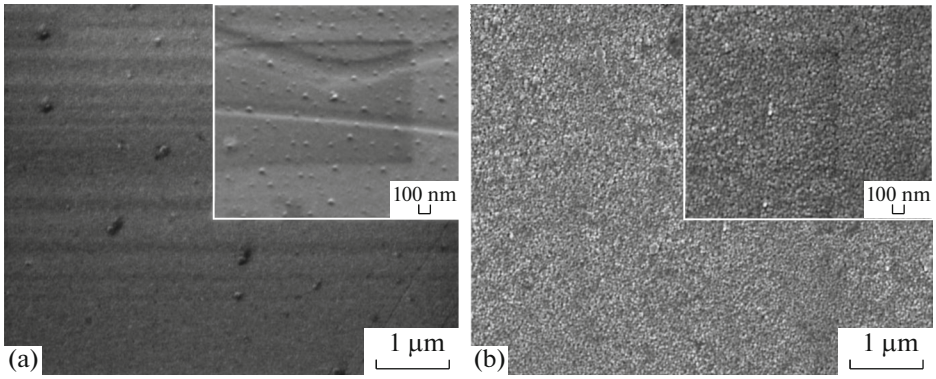

Fig. 3. SEM Micrographs of the TiO_2 thin films annealing at 350°C deposited (a) by sol–gel dip-coating; (b) by sputtering processes.

145 (E_{g1}), 198 (E_{g2}), 397 (B_{1g}), 517 ($B_{1g} + A_{1g}$), and 640 cm^{-1} (E_{g3}). The most intense mode 145 cm^{-1} (E_{g1}) represents the vibrations of oxygen atoms along *c*-axis [1, 18]. These vibrations are assigned to the TiO_2 anatase phase; these results are in good agreement with the data from the literature [1, 14, 15, 19]. As for the micro-Raman spectrum of TiO_2-SG appeared to have no prominent peaks, this sample has amorphous titanium, that's because the temperature is insufficient to move and organize the atoms in a crystalline structure.

Thermal property of the TiO_2-SG samples have been determined by DSC and TGA graphs for a synthesized TiO_2 xerogel powder. Figure 2 shows the results of DSC and TGA analysis of TiO_2 powder.

In the TGA analysis, three weight-loss regions were observed. The significant weight loss is attributed to the evaporation of adsorbed water, the thermal and vaporization decomposition of the organic solvent [20]. The loss weight annealing at 350°C can be explained by the beginning of transformation of amorphous phase to anatase phase with increasing the temperature until 500°C.

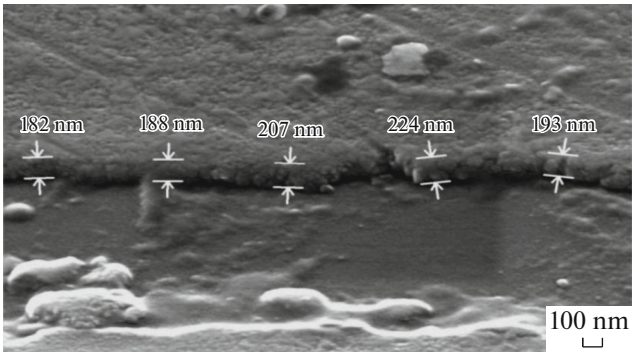

Fig. 4. The cross-section micrograph of the TiO_2 thin films deposited by sputtering process and annealed at 350°C.

3.2. SEM Analysis

The scanning electronic micrographs (SEM) studies showed a clear change in surface morphology of samples at various deposition processes (Fig. 3).

It is obvious that the TiO_2-SG has a uniform smooth and more porous surface with very small, irregular, and not well-formed grains. Which could lead to the amorphous structure, this is clear in micro-Raman spectroscopy. We can see a clear difference in the TiO_2-Sput, the sample is homogeneous and shows uniform distribution of densely packed well-defined grains and the grain size becomes larger. This clearly indicates the crystalline structure, which is anatase phase.

The thickness of TiO_2-Sput thin film was obtained using SEM cross-section as shown in Fig. 4.

In this study, the thickness of the film used was 200 nm. We can see it in M-Line spectroscopy (MLS) measurement.

3.3. Optical Analysis

3.3.1. UV–Visible measurement. The UV–Visible spectra of TiO_2 films fabricated by sputtering and sol-gel processes, annealed at 350°C, and deposited onto glass substrates are recorded in a range of 300–800 nm and shown in Fig. 5.

All the measurements of TiO_2 samples are performed at room temperature, it can be seen that the films have high transparency in the visible region with an overage transmittance varying from 60 to 88%. It marks the transmittance of TiO_2-Sput sample as relatively higher than TiO_2-SG sample.

The optical band gap E_g can be obtained from the transmittance spectra by Tauc's method. The band gap E_g was calculated using the famous Tauc and Beer–Lambert equation [21, 22]:

$$\alpha h\nu = A(h\nu - E_g)^n, \quad (1)$$

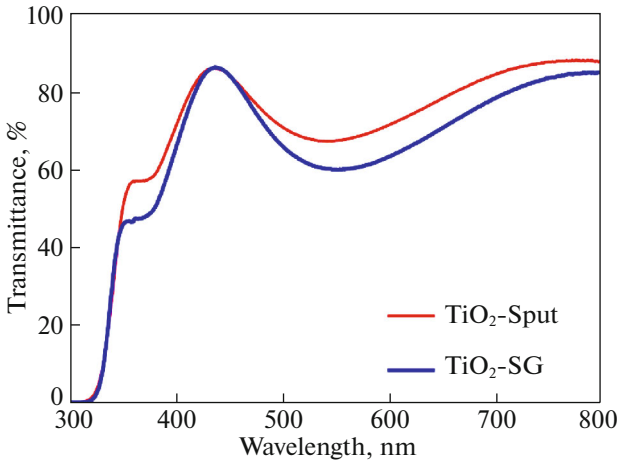

Fig. 5. Transmittance spectra of the TiO_2 thin films elaborated by sol–gel and sputtering processes annealing at 350°C.

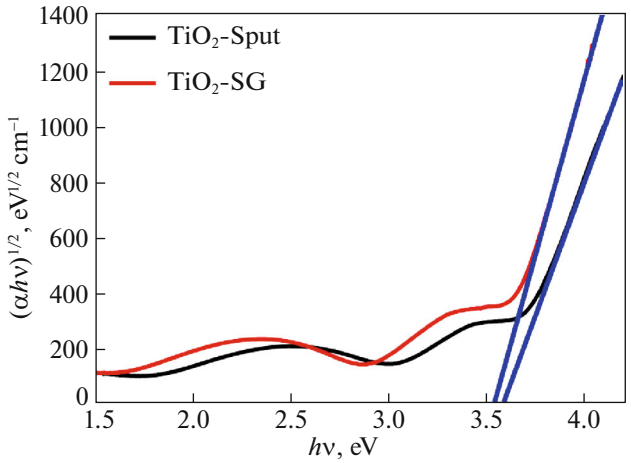

Fig. 6. Tauc plots of the TiO_2 thin films deposited by sol–gel and sputtering processes and annealed at 350°C.

where A is constant of direct transition, $h\nu$ is the photon energy (in eV), and the value of n can be 1/2, 2, 3/2, and 3 depending on whether it is indirect transitions.

Figure 6 shows the optical band gap determined by plotting a graph of $(\alpha h\nu)^{1/2}$ versus $h\nu$ and extrapolation of $(\alpha h\nu)^{1/2}$ by a straight line = 0 to give the optical band gap values of the samples.

The optical band gap values are evaluated as 3.48 and 3.53 eV at TiO_2-SG and TiO_2-Sput, respectively. It can be said that there is relatively increasing in the band gap for the physical method (sputtering) compared to chemical method (sol–gel).

3.3.2. Waveguiding measurements. M-Line spectroscopy (MLS) technique is an optical method uses to obtain the various guided modes and to determine the different opt-geometric parameters (thickness and refractive index) of waveguiding thin films. [23]. Consequently, we can determine the refractive indices n_{TE} (ordinary refractive index) and n_{TM} (extraordinary refractive index) for the transverse electric (TE) and transverse magnetic (TM) polarizations, and the thickness of films (d).

Figure 7 displays the typical TE_0 and TM_0 guided modes spectra for TiO_2-SG and TiO_2-Sput thin films annealed at 350°C.

We notice the excitation of one guided mode for both TE_0 and TM_0 polarization for all TiO_2 samples. From the FWHM of the mode spectra, we can further expect the TiO_2 thin film planar waveguides at both processes. The results of FWHM showed that the TE_0 and TM_0 spectra of TiO_2-SG are sharper than TiO_2-Sput spectra. Our study suggests that the guided mode spectra with smaller FWHM possess lower optical losses and that is what was mentioned in the work of Dehimi et al. [24].

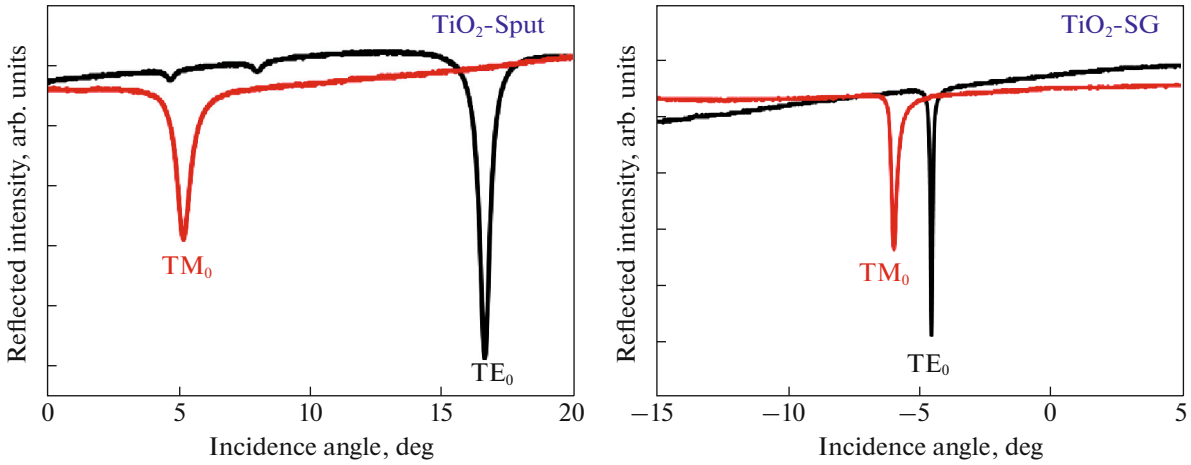

Fig. 7. Typical TE_0 and TM_0 guided mode spectra of TiO_2 thin films deposited by sol–gel and sputtering processes and annealed at 350°C.

Table 1. Summaries of the thicknesses, refractive indices, and porosity of TiO_2 thin films deposited by sol–gel and sputtering techniques and annealed at 350°C

Samples	Thickness d, nm	Effective index $N_0(TE_0)$	Effective index $N_0(TM_0)$	Refraction index n	FWHM TE_0	FWHM TM_0	Porosity, %
TiO_2-Sput	204	2.03	1.88	2.26	0.45	0.61	23.06
TiO_2-SG	216	1.86	1.74	2.06	0.10	0.25	38.85

The porosity ($P(\%)$) of the films is calculated using the formula of Yoldes [25]:

$$P(\%) = \left(1 - \frac{n^2 - 1}{n_b^1 - 1}\right), \quad (2)$$

where n is the refractive index of film without pores and n_b is the refractive index of the porous film. Table 1 summarizes the mean values of refractive index and the thickness of TiO_2 thin films obtained by MLS.

The film was well deposited by reactive sputtering process with relatively uniform grain size distribution and dense morphology throughout the surface, which leads to the increase of refractive index. The values of refractive index for TiO_2 sample are in good agreement with previous works [1, 26]. Our observations suggest that amorphous TiO_2 phase thin films prepared by sol–gel might be a promising candidate for waveguiding applications.

4. CONCLUSIONS

Structural, morphological, and optical properties of TiO_2 thin film grown by sol–gel dip-coating and reactive DC magnetron sputtering processes are studied. The micro-Raman analysis indicates that TiO_2-SG presents an amorphous TiO_2 phase and the vibrational mode of TiO_2-Sput is anatase phase. SEM spectroscopy has shown that TiO_2-SG has a disordered and more porous surface with very small, irregular, and not well formed grains, while TiO_2-Sput sample is homogeneous and shows uniform distribution of densely packed well-defined grains, and the grain size becomes larger. The obtained films have an optical transmission varying from 60 to 88% in the visible region. The forbidden optical band energies, deduced from the transmittance, are 3.48 and 3.53 eV for the TiO_2-SG and TiO_2-Sput films, respectively. The obtained results prove that the TiO_2-SG thin films have more suitable properties of low optical losses because we have low FWHM of the modes TE and TM spectra, and the developed TiO_2-SG thin films can be used in amorphous waveguide applications.

FUNDING

This work is supported by Formation-University Research Project (PRFU) of Algerian ministry of high education and scientific research (nos. BOOL02UN250120200007 and BOOL02UN3001120190006).

CONFLICTS OF INTEREST

The authors declare that they have no conflict of interest.

REFERENCES

1. F. Medjaldi, A. Bouabellou, Y. Bouachiba, A. Taabouche, K. Bouatia, and H. Serrar, Mater. Res. Express **7**, 016439 (2020).
2. H. E. Doghmane, T. Touam, A. Chelouche, F. Challali, and B. Bordji, Semiconductors **54**, 268 (2020).
3. D. A. H. Hanaor and C. C. Sorrell, J. Mater. Sci. **46**, 855 (2011).
4. K. Zakrzewska and M. Radecka, Nanoscale Res. Lett. **12**, 89 (2017).
5. A. Ranjitha, M. Thambidurai, S. Foo, N. Muthukumarasamy, and D. Velauthapillai, Mater. Sci. Energy Technol. **2**, 385 (2019).
6. M. N. Islam and J. Podder, Mater. Sci. Semicond. Process. **121**, 105419 (2021).
7. Y. Zhang, Z. Zhou, and H. Li, Appl. Phys. Lett. **68**, 634 (1996).
8. S. M. H. Qaid, M. Hussain, M. Hezam, M. A. M. Khan, H. Albrithen, H. M. Ghaithan, and A. S. Aldwayyan, Mater. Chem. Phys. **225**, 55 (2019).
9. L. C. Sun and P. Hou, Thin Solid Films **455–456**, 525 (2004).
10. I. Dundar, M. Krichevskaya, A. Katerski, and I. O. Acik, R. Soc. Open Sci. **6**, 181578 (2019).
11. N. Çiçek Bezir, A. Evcin, R. Kayali, M. K. Özen, and G. Balyaci, Acta Phys. Polon. A **132**, 620 (2017).
12. Y. Liang, S. Sun, T. Deng, H. Ding, W. Chen, and Y. Chen, Mater. **11**, 450 (2018).
13. M. R. Alfaro Cruz, D. Sanchez-Martinez, and L. M. Torres-Martínez, Int. J. Hydrogen Energy **44**, 20017 (2019).
14. R. Hazem, M. Izerrouken, A. Cheraitia, and A. Djehlane, Nucl. Instrum. Methods Phys. Res., Sect. B **444**, 62 (2019).

15. D. Komaraiah, E. Radha, J. James, N. Kalarikkal, J. Sivakumar, M. V. Ramana Reddy, and R. Sayanna, J. Lumin. **211**, 320 (2019).

16. R. Taziwa, E. Meyer, and N. Takata, J. Nanosci. Nanotechnol. Res. **1**, 1 (2017).

17. U. Balachandran and N. G. Eror, J. Solid State Chem. **42**, 276 (1982).

18. S. K. Gautam, F. Singh, I. Sulania, R. G. Singh, P. K. Kulriya, and E. Pippel, J. Appl. Phys. **115**, 143504 (2014).

19. F. D. Hardcastle, J. Arkansas Acad. Sci. **65**, 43 (2011).

20. A. Sharma, R. K. Karn, and S. K. Pandiyan, J. Basic Appl. Eng. Res. **1** (9), 1 (2014).

21. J. Tauc, *Amorphous and Liquid Semiconductors* (Plenum, London, 1974).

22. A. S. Hassanien and A. A. Akl, Phys. B (Amsterdam, Neth.) **576**, 411718 (2020).

23. A. Taabouche, A. Bouabellou, F. Kermiche, F. Hanini, C. Sedrati, Y. Bouachiba, and C. Benazzouz, Ceram. Int. **42**, 6701 (2016).

24. M. Dehimi, T. Touam, A. Chelouche, F. Boudjouan, D. Djouadi, J. Solard, A. Fischer, A. Boudrioua, and A. Doghmane, Adv. Condens. Matter Phys. **2015**, 1 (2015).

25. E. Yoldas and P. W. Partlow, Thin Solid Films **129**, 1 (1985).

26. F. Gracia, F. Yubero, J. P. Holgado, J. P. Espinos, A. R. Gonzalez-Elipe, and T. Girardeau, Thin Solid Films **500**, 19 (2006).